



 Cite this: *Phys. Chem. Chem. Phys.*, 2022, 24, 12804

 Received 4th April 2022,
Accepted 13th May 2022

DOI: 10.1039/d2cp01565j

rsc.li/pccp

Nucleophilicity of the boron atom in compounds R–B, (R = F, Cl, Br, I, CN, NC, CH₃, SiH₃, CF₃, H): a new look at the inductive effects of the group R[†]

 Ibon Alkorta ^a and Anthony Legon ^{*b}

Nucleophilicities N_{R-B} of molecules R–B (R = F, Cl, Br, I, CN, NC, CH₃, SiH₃, CF₃, H) are determined from the equilibrium dissociation energies D_e of 70 hydrogen-bonded complexes R–B··HX (X = F, Cl, Br, I, HCN, HCCH, HCP). The change in N_{R-B} relative to N_{H-B} of H–B allows a quantitative measure of the inductive effect I_R of each group R because only the group R affects the electron density associated with the axial non-bonding electron pair carried by the boron in R–B. An alternative definition of I_R , suggested by the strong correlation of the N_{R-B} values with the minimum value σ_{min} of the molecular electrostatic surface potential on the 0.001 e Bohr⁻³ iso-surface along the R–B axis leads to excellent agreement between the two definitions.

The molecule fluoroborylene F–B has a ¹Σ⁺ electronic ground state, is isoelectronic with both CO and N₂, and has been characterized experimentally^{1–3} including *via* its millimeter wave spectrum.⁴ It differs from its two isoelectronic analogues both in its chemical stability and in its considerably lower bond order. A generalized valence bond investigation⁵ concludes that the predominant contribution to the valence-bond description of the molecule is from the Lewis structure that has a single covalent bond, 3 equivalent non-bonding electron pairs on F and one non-bonding pair on the axis at B. The negative end of the electric dipole moment³ is at the B atom, indicating that B is the nucleophilic region of BF. In this article, we report *ab initio* calculations of the geometries and dissociation energies D_e of the 70 hydrogen-bonded complexes R–B··HX, where R is as listed above and X = F, Cl, Br, I, CN, CP or CCH.

The molecules CO and N₂ have featured centrally in the identification and characterization of both hydrogen-bonded interactions with Lewis acids^{6,7} such as HX (X = F, Cl, Br, I, CN,

CCH) and of halogen-bonded complexes with Lewis acids such as XY = ClF, Cl₂, BrCl, Br₂ and ICl.⁸ The electronic structure of B–F, especially the axial non-bonding pair at B, suggests that B–F, like N₂ and CO, will form linear hydrogen-bonded complexes of the type F–B··HX.⁹ Moreover, given that the predominant valence-bond structure of F–B has a single bond, it should be possible to replace F in F–B by other monovalent atoms/groups R, for example, R = H, CH₃, SiH₃, CF₃, Cl, Br, I, CN, NC.

Herein, we examine the effect of the group R on D_e of the R–B··HX complexes and from this determine the nucleophilicity of the boron atom in the various molecules R–B. It has been established elsewhere^{10–12} that the equilibrium dissociation energy D_e of a complex formed by a Lewis base with a Lewis acid *via* a non-covalent interaction (such as a hydrogen bond, a halogen bond, *etc.*) can be written in terms of the nucleophilicity N_{base} of the Lewis base and the electrophilicity E_{acid} of the Lewis acid according to the expression

$$D_e = c'N_{base}E_{acid} \quad (1)$$

For convenience, the constant c' is chosen to be the unit of energy 1.0 kJ mol⁻¹ so that N_{base} and E_{acid} will be dimensionless when D_e is measured in kJ mol⁻¹. Through a least-squares analysis of *ab initio*-calculated D_e values of 250 complexes involving a range of types of non-covalent interaction, a set of N_{base} and E_{acid} values were determined¹² for 11 simple Lewis bases (N₂, CO, HC ≡ CH, CH₂ = CH₂, C₃H₆, PH₃, H₂S, HCN, H₂O, H₂CO and NH₃) and 24 Lewis acids (including most of the series of interest here, namely HF, HCl, HBr, HC ≡ CH, HCN, HCP). The values of E_{HX} for these Lewis acids are set out in Table 1. Note that the value $E_{HBr} = 3.94$ is corrected from the value 4.56 given in ref. 12. It was re-determined from the gradient of the linear regression fit of the D_e versus N_{base} plot for the series of complexes base··HBr, where base = N₂, CO, HC≡CH, CH₂=CH₂, PH₃, H₂S, HCN, H₂O and NH₃. This graph is available as Fig. S1 of the ESI.[†] The previously undetermined value $E_{HI} = 2.77$ was similarly obtained from the linear

^a Instituto de Química Médica (IQM-CSIC). Juan de la Cierva, 3, 28006, Madrid, Spain

^b School of Chemistry, University of Bristol, Cantock's Close, Bristol, BS8 1TS, UK. E-mail: a.c.legon@bristol.ac.uk

[†] Electronic supplementary information (ESI) available: Optimised geometries and energies, Molecular electrostatic potential diagrams of molecules R–B. See DOI: <https://doi.org/10.1039/d2cp01565j>



Table 1 Electrophilicities E_{HX} of Lewis acids HX and equilibrium dissociation energies D_e /(kJ mol⁻¹) for the process R-B...HX = R-B + HX calculated at the CCSD(T)(F12c)/cc-pVDZ-F12 level, with counterpoise correction

Lewis acid HX	E_{HX}	H ₃ C-B	H ₃ Si-B	H-B	F-B	Cl-B	Br-B	I-B	NC-B	CN-B	F ₃ C-B
HF	6.75	40.46	35.82	33.39	21.52	25.59	24.10	23.19	23.07	24.82	21.50
HCl	4.36	26.26	22.92	20.52	12.81	15.73	14.90	14.51	13.49	14.85	12.58
HBr	3.94	23.80	20.79	18.00	10.93	13.72	13.11	12.67	11.57	12.80	10.77
HI	2.77	17.28	14.62	12.59	7.67	9.79	9.31	9.46	8.02	8.99	7.50
HCN	3.71	22.26	18.40	17.28	11.43	13.91	13.03	12.45	10.99	12.81	10.17
HCCH	2.16	11.34	9.54	9.01	6.13	7.24	6.80	6.49	6.22	6.93	5.79
HCP	2.02	11.39	9.60	8.94	6.08	7.28	6.88	6.64	6.13	6.89	5.73

regression fit of the corresponding graph for the base...HI series, also shown in Fig. S1 (ESI†).

The main aim of this report is to measure the nucleophilicity of the molecule R-B as a function of the group R when acting as a hydrogen-bond acceptor at boron. According to eqn (1), if D_e /(kJ mol⁻¹) is plotted on the ordinate against E_{HX} along the abscissa for each of the series of hydrogen-bonded complexes R-B...HX (X = F, Cl, Br, I, CN, CCH, CP), the result for a given R should be a straight line through the origin. The gradient of each such graph yields $N_{\text{R-B}}$ (given that $c' = 1.0$ kJ mol⁻¹). The change in $N_{\text{R-B}}$ with group R is a measure of the change in electron density at the non-bonding pair carried by the B atom and is presumably caused by the differing inductive effects of groups R. Some quantitative definitions of the inductive effects of the groups R based on this work are presented.

The geometries of the 70 complexes were optimized at the CCSD(T) (F12c) computational level^{13,14} with the cc-pVDZ-F12 basis set¹⁵ using the frozen-core approximation and were constrained to have $C_{\infty v}$ or C_{3v} symmetry, as appropriate. The cartesian coordinates of the optimized geometries are available in Table S1 of the ESI.† The dissociation energies D_e were corrected for basis set superposition error (BSSE) using the full counterpoise method of Boys and Bernardi.¹⁶ The calculation were executed with the MOLPRO program.¹⁷ The molecular electrostatic surface potentials (MESP) of the isolated R-B molecules were calculated at the MP2/aug-cc-pVTZ level with the GAUSSIAN program¹⁸ and analyzed on the 0.001 e Bohr⁻³ electron density iso-surface with the multiwfn program.¹⁹ MESP diagrams for all R-B molecules are available in Table S2 ESI.†

The dissociation energies D_e calculated at the CCSD(T)(F12c)/cc-pVTZ-F12 level of theory (after counterpoise correction) for the 10 series of hydrogen-bonded complexes R-B...HX having R = H, CH₃, SiH₃, CF₃, F, Cl, Br, I, CN, NC, where X is one of F, Cl, Br, CN, I, CCH and CP for each R, are included in Table 1.

Graphs of D_e plotted against the electrophilicity E_{HX} of the HX molecule (from Table 1) are set out in three separate figures, for clarity, while each contains the line for H-B...HX, recognizing that H is the usual reference when the inductive effects of different groups R are compared. Included in Fig. 1 are the plots for R = H, F, Cl, Br, I, while those R = H, H₃C and H₃Si are in Fig. 2, and those for R = H, CN, NC, F₃C are in Fig. S2 (ESI†). The gradients and the values of R^2 from linear regression fits of the points for each group R are shown in the inset of

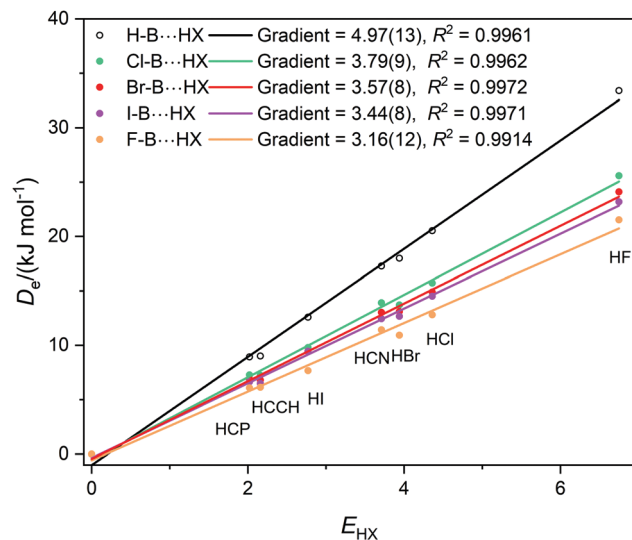


Fig. 1 Graphs of dissociation energy D_e of complexes R-B...HX versus the electrophilicity E_{HX} of the Lewis acid HX for R = H, F, Cl, Br and I.

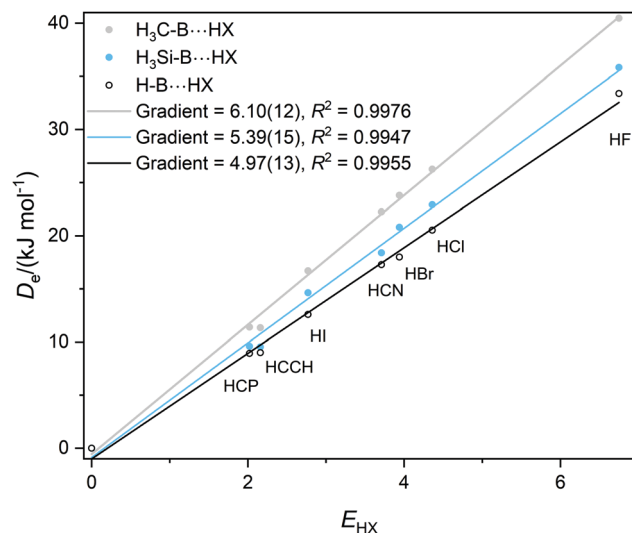


Fig. 2 Graphs of dissociation energy D_e of complexes R-B...HX versus the electrophilicity E_{HX} of the Lewis acids HX for R = H, H₃C- and H₃Si-.

each figure. The quality of the fit for each group R is excellent (as indicated by $R^2 > 0.99$ in all but one case).



Fig. 1 shows clearly that the nucleophilicities N_{R-B} of the R-B molecules- [see eqn (1)] are in the order R = H > Cl > Br ~ I > F. If the inductive effect I_R of a group R relative to H is defined by eqn (2):

$$I_R = (N_{R-B} - N_{H-B}) \quad (2)$$

Then $I_H = 0$, $I_{Cl} = -1.18(22)$, $I_{Br} = -1.40(21)$, $I_I = -1.53(21)$, and $I_F = -1.81(25)$. This definition is consistent with the sign of the inductive effect chosen by Ingold,²⁰ who assigned electron attracting groups, such as halogen atoms, to have a negative inductive effect $-I$.

It is immediately obvious from Fig. 2 that the gradients of the D_e versus E_{HX} graphs for the $H_3C-B \cdots HX$ and $H_3Si-B \cdots HX$ series are greater than that for the $H-B \cdots HX$ series. This indicates that substitution of H by a methyl or a silyl group pushes electron density onto B relative to H. According to the definition given in eqn (2) the inductive effect I_R of the group H_3C- is $I_{H_3C} = +1.13(25)$ and that of H_3Si- is $I_{H_3Si} = +0.42(28)$. Thus, both groups exhibit a positive inductive effect, although the range of each value transmitted from the errors in the gradients is larger than ideal.

The corresponding graphs of D_e versus E_{HX} for the series R-B \cdots HX when R- is H-, CN- (isocyanide), NC- (cyanide), and F_3C- (trifluoromethyl) are available in the ESI† as Fig. S2. The last three groups R are electron-withdrawing relative to H. In fact, the gradients of the graphs for R = F_3C- (Fig. 3) and R = F- (Fig. 1) are the same. Given the definition $I_R = N_{R-B} - N_{H-B}$ in eqn (2) the inductive effects are $I_{F_3C} = -1.82(27)$, $I_{NC} = -1.32(25)$ and $I_{CN} = -1.56(26)$. Thus, the electron-withdrawing effects of the CF_3 group and the F atom are identical, while the cyanide group is a better electron-withdrawing group than isocyanide and has a value I_{CN} comparable with that of Br or I. Unfortunately, the errors in the fitted D_e versus the E_{HX} straight lines are

sufficient that more precise values of the inductive effects I_R of the groups R cannot be obtained by the present approach.

In conclusion, we have shown that by calculating the equilibrium dissociation energies D_e for the series of hydrogen-bonded complexes R-B \cdots HX, where X = F, Cl, Br, I, HCN, HCCH and HCP, it is possible to determine the nucleophilicity N_{R-B} of the axially symmetric molecules R-B. Repeating this procedure for each group in the series R = H_3C , H_3Si , H-, F-, Cl-, Br-, I-, CN-, NC-, and F_3C- shows that, relative to H-, the groups H_3C- and H_3Si- increase the nucleophilicity of the B atom in forming hydrogen bonds with HX, while the halogen atoms, the pseudo-halogens CN- and NC-, and the fully fluorinated methyl group, withdraw electronic charge from the non-bonding electron pair carried by boron. The change $N_{R-B} - N_{H-B}$ in the nucleophilicity of the axial, non-bonding electron pair on B in molecules R-B relative to H-B thus, in principle, provides a clean method of assessing the inductive effect I_R of the group R. This approach has the advantage that the molecular complexes R-B \cdots HX are isolated from solvent effects, that the group R is directly attached to the boron atom and the changes in the D_e values when R is changed result directly from the changes in electron density in the non-bonding pair carried by B.

Politzer and co-workers^{21,22} showed some time ago that electrostatic potentials can also be related to nucleophilic processes. A useful, recent general discussion²³ of molecular electrostatic surface potentials (MESPs) is available from the same group. We now examine the relationship between MESPs and the inductive effect.

The molecular electrostatic surface potential (MESP) calculated at the MP2/aug-cc-pVTZ level on the 0.001 e Bohr⁻³ iso-surface (in particular, the value σ_{min} on the R-B molecular axis near to the boron atom) provides a measure of the change in electrostatic potential at the non-bonding electron pair carried by B when the group R is changed.

The values of σ_{min} for the 10 compounds R-B (R = H_3C- , H_3Si- , H-, F-, Cl-, Br-, I-, CN-, NC-, and F_3C-) are collected in Table 2. Fig. 3 displays a graph of N_{R-B} versus σ_{min} . It is clear from Fig. 3 that there is a strong correlation between the two last-named quantities. Indeed, this suggests another way to express the inductive effect I'_R of group R, namely by the equation:

$$I'_R = \{\sigma_{min}(R-B) - \sigma_{min}(H-B)\} / \{\sigma_{min}(H-B)\} \quad (3)$$

where division by $\sigma_{min}(H-B)$ ensures a dimensionless quantity that is normalised with respect to the value for H-B. The I'_R so calculated from the $\sigma_{min}(R-B)$ are included in Table 2.

The values determined from the nucleophilicities ($N_{R-B} - N_{H-B}$), but normalised according to the value of N_{H-B} , to give

$$I_R^{norm} = (N_{R-B} - N_{H-B}) / N_{H-B} \quad (4)$$

are included in Table 2 and allow a more strict comparison. The conclusion of interest from Table 2 is that whichever of the two definitions of the inductive effect presented here is used, the values in the two scales are very similar. The linear correlation

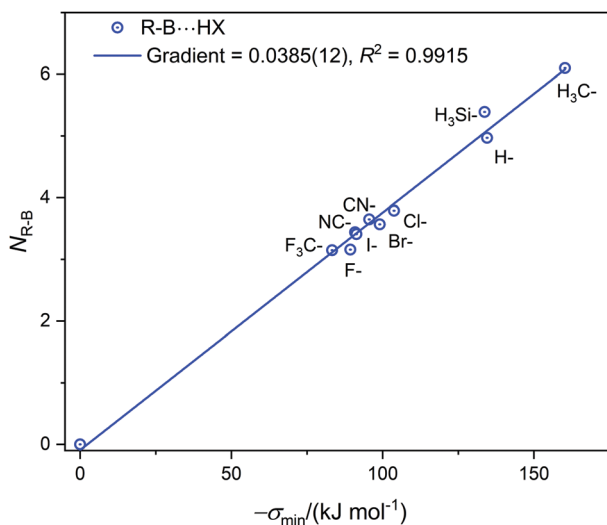


Fig. 3 The nucleophilicities N_{R-B} of molecules R-B (determined from the gradient of the D_e versus E_{HX} graphs in Fig. 1, 2 and Fig. S2, ESI†) plotted against σ_{min} (the minimum value of the electrostatic potential on the 0.001 e Bohr⁻³ iso-surface of R-B on the molecular axis at the boron atom).



Table 2 Comparison of three methods of measuring the inductive effect of monovalent groups R

Group R	σ_{\min} (R-B) ^a kJ mol ⁻¹	Inductive effect I_R^{norm} ^b	Inductive effect I'_R ^c	Hammett σ constant ^d
H ₃ C-	-160.3	0.23	0.19	-0.17
H ₃ Si-	-133.7	0.08	-0.01	0.10
H-	-134.5	0.00	0.00	0.00
F-	-89.3	-0.36	-0.34	0.06
Cl-	-103.7	-0.24	-0.23	0.23
Br-	-99.0	-0.28	-0.26	0.23
I-	-90.9	-0.31	-0.32	0.18
NC-	-91.4	-0.31	-0.32	0.66
CN-	-95.5	-0.27	-0.29	0.49
F ₃ C-	-83.3	-0.37	-0.38	0.54

^a Value of the MESP on the 0.001 e Bohr⁻³ iso-surface on the R-B molecular axis at boron. ^b As defined in eqn (4). ^c As defined by eqn (3). ^d The Hammett σ substituent constants for the para-position of benzoic acid [24]. They are positive for electron withdrawing groups and negative electron donating groups, relative to hydrogen.

between the two sets of parameters, I_R^{norm} and I'_R , has $R^2 = 0.983$, a slope close to one (0.90), and an intercept near to zero (-0.032). Finally, the Hammett σ substituent constant is commonly cited²⁴ as a measure of the relative inductive effects of groups R attached to, for example, benzoic acid and is based on how equilibrium constants for dissociation of the acid are affected by substituents R at the *para*- and *meta*-positions of the benzene ring. The values for the *para*-position are included in Table 2 and, after noting they are of opposite sign from the I_R proposed here, the magnitudes are in only fair agreement with those of the I_R introduced here, but the Hammett constant applies to equilibria/chemical reactions in solvents, and are therefore not strictly comparable.

Conflicts of interest

There are no conflicts to declare.

Acknowledgements

ACL thanks the University of Bristol for a Senior Research Fellowship. IA thanks the Ministerio de Ciencia e Innovación of Spain (PGC2018-094644-B-C22 and PID2021-125207NB-C32) and Comunidad de Madrid (P2018/EMT-4329 AIRTEC-CM) for financial support.

Notes and references

- 1 D. L. Hildenbrand and E. Murad, *J. Chem. Phys.*, 1965, **43**, 1400–1403.
- 2 P. L. Timms, *J. Am. Chem. Soc.*, 1967, **89**, 1629–1632.
- 3 D. Vidovic and S. Aldridge, *Chem. Sci.*, 2011, **2**, 601–608.
- 4 G. Cazzoli, L. Cludi, C. Degli Esposti and L. Dore, *J. Mol. Spectrosc.*, 1989, **134**, 159–167.
- 5 F. Fantuzzi, T. M. Cardozo and M. A. C. Nasimento, *J. Phys. Chem. A*, 2014, **119**, 5335–5343.
- 6 A. C. Legon, P. D. Soper, M. R. Keenan, T. K. Minton, T. J. Balle and W. H. Flygare, *J. Chem. Phys.*, 1980, **73**, 583–584.
- 7 P. D. Soper, A. C. Legon, W. G. Read and W. H. Flygare, *J. Chem. Phys.*, 1982, **76**, 292–300.
- 8 A. C. Legon, *Angew. Chem., Int. Ed.*, 1999, **38**, 2686–2714.
- 9 I. Rozas, I. Alkorta and J. Elguero, *J. Phys. Chem. A*, 1999, **103**, 8861–8869.
- 10 A. C. Legon and D. J. Millen, *J. Am. Chem. Soc.*, 1987, **109**, 356–358.
- 11 A. C. Legon, *Phys. Chem. Chem. Phys.*, 2014, **16**, 12415–12421, see Correction 2014, **16**, 25199–25199.
- 12 I. Alkorta and A. C. Legon, *Molecules*, 2017, **22**, 1786–1799.
- 13 C. Hättig, D. P. Tew and A. Köhn, *J. Chem. Phys.*, 2010, **132**, 231102.
- 14 C. Hättig, W. Klopper, A. Köhn and D. P. Tew, *Chem. Rev.*, 2012, **112**, 4–74.
- 15 J. G. Hill and K. A. Peterson, *J. Chem. Phys.*, 2014, **141**, 094106.
- 16 S. F. Boys and F. Bernardi, *Mol. Phys.*, 1970, **19**, 553–566.
- 17 H.-J. Werner, P. J. Knowles, G. Knizia, F. R. Manby and M. Schütz, *Wiley Interdiscip. Rev.: Comput. Mol. Sci.*, 2012, **2**, 242–253.
- 18 M. J. Frisch, G. W. Trucks, H. B. Schlegel, G. E. Scuseria, M. A. Robb, J. R. Cheeseman, G. Scalmani, V. Barone, G. A. Petersson and H. Nakatsuji, *et al.*, *Gaussian 16; Revision, A.03*, Gaussian, Inc.: Wallingford, CT, USA, 2016.
- 19 T. Lu and F. Chen, *J. Comput. Chem.*, 2012, **33**, 580–592.
- 20 C. K. Ingold, *Structure and Mechanism in Organic Chemistry*, Cornell University Press, Ithaca, New York, 1953, p. 71.
- 21 J. S. Murray and P. Politzer, *Chem. Phys. Lett.*, 1988, **152**, 364–370.
- 22 P. Sjöberg and P. Politzer, *J. Chem. Phys.*, 1990, **94**, 3959–3961.
- 23 J. S. Murray and P. Politzer, *WIREs Comput. Mol. Sci.*, 2017, **7**, e1326.
- 24 C. Hansch, A. Leo and R. W. Taft, *Chem. Rev.*, 1991, **91**, 165–195.

